

論文内容の要旨

論文題目：

Three-Dimensional Dirac Electron Systems in the
Family of Inverse-Perovskite Material Ca_3PbO

(逆ペロブスカイト Ca_3PbO とその類似物質
における 3次元ディラック電子系)

氏名 荻宿 俊風

In this thesis, cubic inverse perovskite material Ca_3PbO and its family (A_3EO with $\text{A}=\text{Ca}$, Sr , Ba and $\text{E}=\text{Pb}$, Sn) are theoretically proposed as new candidates for Dirac electron systems by the first-principles band calculation. Then, we construct a simple tight-binding model describing the low-energy band structure. The origin of the Dirac electron in Ca_3PbO series is clarified by analyzing the constructed tight-binding model. Some physical properties, the orbital magnetic susceptibility and the surface band structure, are investigated using the tight-binding model in order to elucidate the characters associated with the Dirac electrons in Ca_3PbO series.

The crystal structure of the target material Ca_3PbO is depicted in Fig. 1. It is an “inverse” perovskite structure in which a nonmetallic atom (O, in this case) is surrounded by metallic atoms (Ca, in this case) octahedrally.

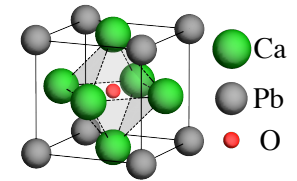


Fig. 1: Crystal structure.

First, the band structure of Ca_3PbO is investigated by means of the first-principles density functional theory (DFT). The crystal parameters required in the calculation are taken from the experiments. The calculated band structure is shown in Fig. 2(a). In the shown energy range, the bands below the Fermi energy are mainly originated from the Pb $6p$ orbitals, while the entangled bands above the Fermi energy are mainly originated from the Ca $3d$ orbitals. However, note that the top of the p-bands (bands originated from the Pb $6p$ orbitals) is located above the bottom of the d-bands (bands originated from the Ca $3d$ orbitals). This feature is important for the emergence of the Dirac electron in Ca_3PbO as described later.

The most interesting point in the obtained band structure is that there exists a tilted anisotropic three-dimensional massive Dirac electron. A Dirac point, which is defined as a center of linear

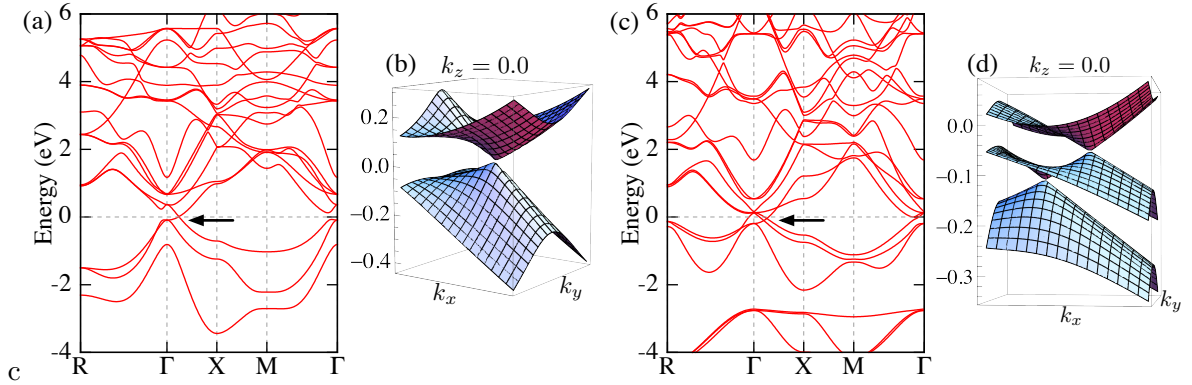


Fig. 2: (a,c) The band structures of Ca_3PbO and Ba_3SnO . (b,d) The dispersion relations around the Dirac points in Ca_3PbO and Ba_3SnO .

dispersion of Dirac electron, is located exactly at the Fermi energy and on the Γ -X line in the cubic Brillouin zone. Figure 2(b) shows the dispersion relation around the Dirac point. We can see the linear dispersion, which is characteristic for a Dirac electron. The existence of a Dirac point on the Γ -X line implies that there are six symmetrically equivalent Dirac points due to the cubic symmetry of the system. Within the first-principles calculation, the mass gap and the velocity characterizing the Dirac electron are estimated as 15 meV and $2\text{-}4 \times 10^5$ m/s, respectively. Note that the velocity depends on the direction. Using these values, the effective cyclotron mass for this Dirac electron becomes as small as 10^{-2} of the bare electron mass. The strong magnetic response is expected due to the smallness of the effective cyclotron mass.

We also discuss the relation to the other three-dimensional Dirac electron systems and the topological properties of Ca_3PbO . Although Ca_3PbO is proved to be not a topological insulator, it is worth noting that Ca_3PbO has some commonalities with a topological insulator such as a strong spin-orbit coupling and an “inverted” band structure.

The band structures of the families of Ca_3PbO are also studied by the first-principles calculation. We find that Sr_3PbO , Ba_3PbO , Ca_3SnO , and Sr_3SnO have band structures similar to Ca_3PbO near the Fermi energy. There appear Dirac electrons also in these materials. The parameters characterizing Dirac electrons (mass gap, velocity, tilting angle, and anisotropy) differ in each material. For instance, the Sn-based compounds have smaller mass gaps than the Pb-based compounds. This result suggests that it may be possible to control the size of mass gap by fabricating the alloys like $\text{Ca}_3(\text{Pb}_{1-x}\text{Sn}_x)\text{O}$. On the other hand, it turns out that another A_3EO compound Ba_3SnO has a highly distinct dispersion relation near the Fermi energy compared with Ca_3PbO [Figs. 2(c) and 2(d)]. Interestingly, Ba_3SnO has two Dirac points appearing side by side in the energy and the momentum space. These two Dirac points are located near the Fermi energy and on the Γ -X line. Note that the existence of two Dirac points on the Γ -X line implies that there are 12 Dirac points in the whole Brillouin zone due to the cubic symmetry of the crystal. The discovered “twin” Dirac electrons show a peculiar dispersion relation such that the upper Dirac cone of the lower Dirac electrons is continuously deformed into the lower Dirac cone of the upper Dirac electrons [Fig. 2(d)]. Due to this peculiar dispersion relation, if the chemical potential in Ba_3SnO is finely controlled in some way, the shapes of Fermi surfaces

show an interesting evolution.

Next, we construct a simple tight-binding model describing the band structure of Ca_3PbO around the Fermi energy. This study is done for 1) obtaining insights into the emergence of the Dirac electron in Ca_3PbO series and 2) calculating some physical quantities based on the constructed tight-binding model. In order to construct a tight-binding model, we first assign the orbitals to be included in the basis set by analyzing the orbital-weight distribution on the bands obtained in the first-principles calculation. It turns out that three $6p$ orbitals on the Pb atom and three $3d$ orbitals on the three Ca atoms in a unit cell are necessary in constructing a satisfactory tight-binding model. Since the spin-orbit coupling on the Pb atom is strong, the spin degrees of freedom should be explicitly treated. This means that we have 12 ($= (3 + 3) \times 2$) orbitals in the basis set for the tight-binding model. The matrix elements between these 12 orbitals are derived considering the symmetries of the orbitals. The parameters such as the energy levels of basis orbitals, hopping integrals, and the strength of spin-orbit coupling are determined with the help of the maximally localized Wannier functions. Then, we can successfully reproduce the band structure of Ca_3PbO obtained in the first-principles calculation with a simple tight-binding model. It is also possible to construct a model for Ba_3SnO , which has twin Dirac electrons in its band structure, with the same tight-binding model as Ca_3PbO using a different set of the parameters. However, we must note that the Dirac electron in this tight-binding model is exactly massless, while it should be massive according to the first-principles calculation. This point will be discussed later.

After constructing the tight-binding model, we study the parameter dependence of the band structure in order to elucidate which parameter is essential for the emergence of Dirac electrons in this model. Through this investigation, it is clarified that the overlap between the p- and d-bands and the spin-orbit coupling play crucial roles in generating the Dirac electron in this model. Namely, if there is no overlap between the p- and d-bands, the Dirac electron never appears in this model. On the other hand, in the zero spin-orbit coupling limit, there still exists a linear dispersion. However, the low-energy effective Hamiltonian for this case is not a Dirac Hamiltonian.

In order to verify explicitly that the low-energy limit of the effective Hamiltonian for Ca_3PbO takes really a form of a Dirac Hamiltonian, the tight-binding model described above is further analyzed. Applying a proper basis transformation and expanding the matrix elements in the series of the momentum k measured from a Dirac point, it is confirmed that the low-energy limit of the effective Hamiltonian is a Dirac Hamiltonian. After checking that the low-energy effective model is really a Dirac Hamiltonian, we discuss the origin of the Dirac electron in this model. As we have already stated, the overlap between the p- and d-bands is important. In addition to that, it becomes clear that the symmetry of the crystal and the involved orbitals are also important for the emergence of the Dirac electrons in this model. Using the information extracted from all the above arguments, we propose a minimal model describing the Dirac electrons in Ca_3PbO series. Analysis of this minimal model clarifies the role of the spin-orbit coupling for the emergence of the Dirac electrons.

As we have pointed out, the tight-binding model gives a massless Dirac electron. Actually, the small but finite mass term observed in the first-principles calculation can be generated by considering the extra orbitals that are not included in the basis set of the tight-binding model.

Note that newly considered extra orbitals are located far from the Fermi energy. The fact that the finite mass term requires the inclusion of the orbitals far from the Fermi energy ensures the smallness of the mass term.

In general, Dirac electron systems show distinct phenomena when a magnetic field is applied or the translational symmetry is broken. Then, we study the orbital magnetic susceptibility and the surface band structure using the tight-binding model introduced above as a representative magnetic field effect and as a typical broken translational symmetry effect.

The orbital magnetic susceptibility is calculated using the gauge invariant single line formula

$$\chi = \frac{e^2}{\hbar^2} \frac{T}{2N} \sum_{nk} \text{Tr} \left[\hat{v}_x \hat{G} \hat{v}_y \hat{G} \hat{v}_x \hat{G} \hat{v}_y \hat{G} + \frac{1}{2} (\hat{v}_{xy} \hat{G} \hat{v}_x \hat{G} \hat{v}_y \hat{G} + \hat{v}_{xy} \hat{G} \hat{v}_y \hat{G} \hat{v}_x \hat{G}) \right]$$

derived for a tight-binding model. (Derivation is given as an appendix of this thesis.) The calculated results show that the model for Ca_3PbO gives a large diamagnetic susceptibility when the chemical potential is close to the energy of the Dirac point. On the other hand, in the model for Ba_3SnO , the orbital magnetic susceptibility shows two large negative (diamagnetic) peaks as a function of the chemical potential. This is because the twin Dirac electrons exist in Ba_3SnO . In both cases, the orbital magnetic susceptibility sharply depends on the chemical potential and temperature. This property can be used to confirm the existence of Dirac electrons experimentally.

The surface band structures are calculated by using slablike structures with several types of surfaces. For all of the 001, 101, and 111 surfaces, we find nontrivial surface bands that cannot be explained from the bulk bands projected to the surface Brillouin zone. It is worth noting that these surface bands do not have Kramers degeneracy, due to the strong spin-orbit coupling in the model and the broken translational symmetry at the surface. It is an interesting subject to study the relation between the surface states of Ca_3PbO and those of a topological insulator.